

Femtosecond-laser-inscribed sampled fiber Bragg grating with ultrahigh thermal stability

Congzhe Zhang,^{1,2} Yuanhong Yang,¹ Chao Wang,² Changrui Liao,^{2,4} and Yiping Wang^{2,3}

¹Department of Opto-electronics Engineering, School of Instrument Science and Opto-electronics Engineering, Beihang University, Beijing 100191, China

²Key Laboratory of Optoelectronic Devices and Systems of Ministry of Education/Guangdong Province, Shenzhen University, Shenzhen 518060, China

³ypwang@szu.edu.cn

⁴cliao@szu.edu.cn

Abstract: We have successfully fabricated a series of sampled fiber Bragg gratings with easily adjustable sampling periods and duty cycles using an 800 nm femtosecond laser point-by-point inscription. The thermal stability of the fabricated fiber gratings was investigated using isochronal annealing tests, which indicated that the fiber gratings are capable of maintaining high reflectivity at temperatures of up to 1000°C for 8 h. This demonstrates the potential of the developed sampled fiber Bragg gratings for use in multi-wavelength fiber lasers and a variety of high temperature applications.

©2016 Optical Society of America

OCIS codes: (060.3735) Fiber Bragg gratings; (320.7140) Ultrafast processes in fibers; (060.3510) Lasers, fiber; (230.4000) Microstructure fabrication.

References and links

1. H. Lee and G. P. Agrawal, "Add-drop multiplexers and interleavers with broad-band chromatic dispersion compensation based on purely phase-sampled fiber gratings," *IEEE Photonics Technol. Lett.* **16**(2), 635–637 (2004).
2. X. Shu, B. A. L. Gwandu, Y. Liu, L. Zhang, and I. Bennion, "Sampled fiber Bragg grating for simultaneous refractive-index and temperature measurement," *Opt. Lett.* **26**(11), 774–776 (2001).
3. B.-O. Guan, H.-Y. Tam, X.-M. Tao, and X.-Y. Dong, "Simultaneous strain and temperature measurement using a superstructure fiber Bragg grating," *IEEE Photonics Technol. Lett.* **12**(6), 675–677 (2000).
4. J. Yang, S. C. Tjin, and N. Q. Ngo, "Multiwavelength tunable fiber ring laser based on sampled chirp fiber Bragg grating," *IEEE Photonics Technol. Lett.* **16**(4), 1026–1028 (2004).
5. M. Li, X. Chen, T. Fujii, Y. Kudo, H. Li, and Y. Painchaud, "Multiwavelength fiber laser based on the utilization of a phase-shifted phase-only sampled fiber Bragg grating," *Opt. Lett.* **34**(11), 1717–1719 (2009).
6. W. Jin, S. Murray, D. Pinchbeck, G. Stewart, and B. Culshaw, "Absorption measurement of methane gas with a broadband light source and interferometric signal processing," *Opt. Lett.* **18**(16), 1364–1366 (1993).
7. F. Tong, W. Jin, D. Wang, and P. Wai, "Multiwavelength fibre laser with wavelength selectable from 1590 to 1645 nm," *Electron. Lett.* **40**(10), 594–595 (2004).
8. B.-O. Guan, H.-Y. Tam, X. Tao, and X.-Y. Dong, "Highly stable fiber Bragg gratings written in hydrogen-loaded fiber," *IEEE Photonics Technol. Lett.* **12**(10), 1349–1351 (2000).
9. X. Fang, X. Y. He, C. R. Liao, M. Yang, D. N. Wang, and Y. Wang, "A new method for sampled fiber Bragg grating fabrication by use of both femtosecond laser and CO₂ laser," *Opt. Express* **18**(3), 2646–2654 (2010).
10. A. Martinez, M. Dubov, I. Khrushchev, and I. Bennion, "Direct writing of fibre Bragg gratings by femtosecond laser," *Electron. Lett.* **40**(19), 1170–1172 (2004).
11. A. Martinez, I. Khrushchev, and I. Bennion, "Thermal properties of fibre Bragg gratings inscribed point-by-point by infrared femtosecond laser," *Electron. Lett.* **41**(4), 176–178 (2005).
12. G. D. Marshall, R. J. Williams, N. Jovanovic, M. J. Steel, and M. J. Withford, "Point-by-point written fiber-Bragg gratings and their application in complex grating designs," *Opt. Express* **18**(19), 19844–19859 (2010).
13. R. J. Williams, C. Voigtländer, G. D. Marshall, A. Tünnermann, S. Nolte, M. J. Steel, and M. J. Withford, "Point-by-point inscription of apodized fiber Bragg gratings," *Opt. Lett.* **36**(15), 2988–2990 (2011).
14. C. Wang, W. Jin, W. Jin, J. Ju, J. Ma, and H. L. Ho, "Evanescent-field photonic microcells and their applications in sensing," *Measurement* **79**, 172–181 (2015).
15. C. Koutsides, E. Davies, K. Kalli, M. Komodromos, T. Allsop, D. J. Webb, and L. Zhang, "Superstructure fiber gratings via single step femtosecond laser inscription," *J. Lightwave Technol.* **30**(8), 1229–1236 (2012).

16. G. Ehret, C. Kiemle, W. Renger, and G. Simmet, "Airborne remote sensing of tropospheric water vapor with a near-infrared differential absorption lidar system," *Appl. Opt.* **32**(24), 4534–4551 (1993).
17. G. Ehret, C. Kiemle, M. Wirth, A. Amediek, A. Fix, and S. Houweling, "Space-borne remote sensing of CO₂, CH₄, and N₂O by integrated path differential absorption lidar: a sensitivity analysis," *Appl. Phys. B* **90**(3-4), 593–608 (2008).
18. Y. Lai, K. Zhou, K. Sugden, and I. Bennion, "Point-by-point inscription of first-order fiber Bragg grating for C-band applications," *Opt. Express* **15**(26), 18318–18325 (2007).
19. T. Erdogan, "Fiber grating spectra," *J. Lightwave Technol.* **15**(8), 1277–1294 (1997).
20. B. J. Eggleton, F. Ouellette, L. Poladian, and P. A. Krug, "Long periodic superstructure Bragg gratings in optical fibres," *Electron. Lett.* **30**(19), 1620–1622 (1994).
21. M. Ibsen, M. K. Durkin, M. J. Cole, and R. I. Laming, "Sinc-sampled fiber Bragg gratings for identical multiple wavelength operation," *IEEE Photonics Technol. Lett.* **10**(6), 842–844 (1998).
22. C. R. Liao, T. Y. Hu, and D. N. Wang, "Optical fiber Fabry-Perot interferometer cavity fabricated by femtosecond laser micromachining and fusion splicing for refractive index sensing," *Opt. Express* **20**(20), 22813–22818 (2012).
23. C. Liao, S. Liu, L. Xu, C. Wang, Y. Wang, Z. Li, Q. Wang, and D. N. Wang, "Sub-micron silica diaphragm-based fiber-tip Fabry-Perot interferometer for pressure measurement," *Opt. Lett.* **39**(10), 2827–2830 (2014).
24. Y. Li, C. R. Liao, D. N. Wang, T. Sun, and K. T. V. Grattan, "Study of spectral and annealing properties of fiber Bragg gratings written in H₂-free and H₂-loaded fibers by use of femtosecond laser pulses," *Opt. Express* **16**(26), 21239–21247 (2008).
25. C. Liao and D. Wang, "Review of femtosecond laser fabricated fiber Bragg gratings for high temperature sensing," *Photon. Sens.* **3**(2), 97–101 (2013).
26. Y. Li, W. Chen, H. Wang, N. Liu, and P. Lu, "Bragg gratings in all-solid Bragg photonic crystal fiber written with femtosecond pulses," *Lightwave Technology Journalism* **29**, 3367–3371 (2011).

1. Introduction

Sampled fiber Bragg gratings (SFBGs) have attracted recent interest owing to their wide use in a variety of applications such as dense wavelength-division-multiplexed (DWDM) systems [1], fiber-optic sensors [2,3], and multi-wavelength fiber lasers [4,5]. SFBGs generate several equal-spaced reflection wavelength and these can provide more transmission channels in optical fiber communications or multiply the sensitivity of detection [6,7]. The SFBGs can be generated by inducing an amplitude and/or phase modulation in the refractive index of the fiber core, and the resultant reflection spectrum is a sampling function of this modulation. The modulation can be induced by illuminating the fiber segmentally through a phase mask with ultraviolet light or by adding a specially designed amplitude mask during the inscription process [2,8]. However, these methods may be affected by the apodization arising from multiple exposures or may be restricted by the amplitude mask. Fang et al. demonstrated SFBG fabrication by heating a uniform fiber Bragg grating (FBG) inscribed by a femtosecond laser [9]. This method has an optional modulation envelop, but the thermal stability of the resulting SFBGs is limited by the heating process. Point-by-point (PBP) inscription of FBGs offers a remarkable technological flexibility, and the resulting gratings demonstrate good high-temperature stability [10,11]. This fabrication method eliminates the requirement of a phase mask, and the grating parameters can be easily altered by adjusting fiber motion. SFBGs fabricated by PBP inscription were firstly reported by Marshall et al. [12], and the PBP inscription method has demonstrated a remarkable facility for fabricating SFBGs as well as many other types of gratings with customized grating periods, amplitudes, and phases according to specific customer requirements [12–15]. However, the thermal stabilities of these SFBGs were not investigated in these studies.

Having access to gratings with better thermal stability is essential for creating high-power fiber lasers which may be used in differential absorption lidar based remote gas sensing technique [16,17]. The work reported in this paper therefore focuses on the thermal stability of SFBGs fabricated by PBP inscription using an 800 nm femtosecond (fs) laser. The resulting SFBGs exhibit remarkable thermal stability at high temperatures of up to 1000°C, which represents a significant improvement relative to SFBGs inscribed by means of an excimer laser [2,8].

2. Methods

2.1 Experimental setup

A schematic diagram of the fs-laser PBP inscription system employed in the present study is shown in Fig. 1(a), which utilizes a regenerative amplified and low repetition rate Solstice® Ti:sapphire fs laser (Spectra-Physics®, Newport Corp.) with 100 fs pulses, a central wavelength of 800 nm, and a repetition rate of 1 kHz to produce fiber gratings. The laser energy can be attenuated by rotating a half-wave plate with respect to a subsequent Glan-Laser polarizer. The laser beam is focused by means of an oil-immersed 100 × microscope objective with a numerical aperture of 1.25. An SH05 optical beam shutter (Thorlabs, Inc.) is mounted in the light path to eliminate laser irradiation when required. A single-mode optical fiber (Corning SMF-28e) is clamped on a three-axis linear translation stage comprised of a GTS150 linear stage, XMS50 linear stage, and a GTS30V vertical stage (Newport Corp.) to achieve precise three-axis displacement. An image of the optics and translation stage is given in Fig. 1(b).

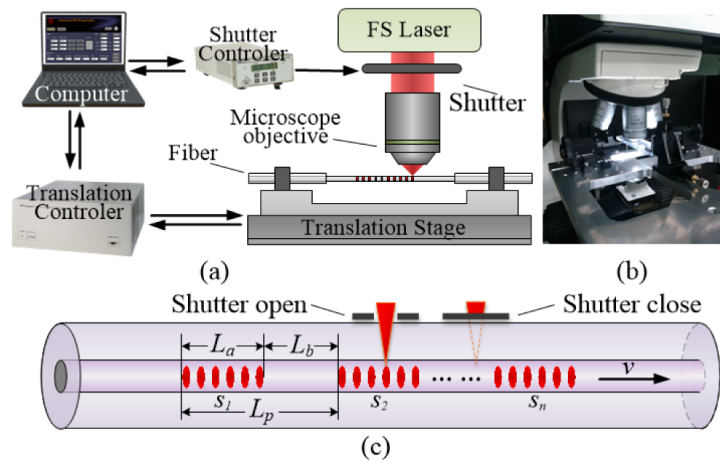


Fig. 1. (a) Schematic diagram of the fs-laser PBP inscription system. (b) Photograph of the fs-laser micropositioning setup. (c) Principle of the SFBG PBP inscription process.

Figure 1(c) illustrates the working principle of PBP inscription employed here for fabrication of SFBGs. Firstly, the laser beam is focused at the center of the fiber core, and then the fiber is translated along the horizontal direction perpendicular to the pulsed laser beam with a desired velocity (v) while the shutter is periodically cycled through open and shut positions. With the shutter open, fs laser pulses irradiate the fiber core, and induce periodical refractive index modulation at the focal point, with a periodicity established according to the value of v . Conversely, laser modulation of the refractive index is removed with the shutter closed. After several switching cycles, a portion of an SFBG is quickly obtained, which is comprised of short grating sections S_1, S_2, \dots, S_n . The lengths of the laser-modulated and un-modulated regions are respectively denoted by L_a and L_b , which define the sampling period ($L_p = L_a + L_b$), and can be adjusted by changing the switching period and duty cycle T of the shutter, where $T = L_a/L_p$. The total length of the SFBG (L) is determined by L_p and the number of sampling sections (N).

2.2 Experimental and simulation results and discussion

Figure 2 shows an optical microscope image of an SFBG fabricated according to the described process. During inscription, v was set to 1.07 mm/s, which, in conjunction with the 1 kHz repetition rate, results in a grating pitch of 1.07 μm , corresponding to a central Bragg

resonance wavelength of ~ 1550 nm. For $L = 8.0$ mm, N and T are set as 10 and 0.20, respectively. To suppress cladding mode coupling, an fs laser energy of ~ 200 nJ was employed, which is slightly lower than that utilized for uniform FBG inscription. In Fig. 2, the measured values of L_p and L_a are $815 \mu\text{m}$ and $168 \mu\text{m}$, respectively. The small difference between the set value of T and the measured value (i.e., 0.21) can be explained by the internal delay of the shutter, which can be eliminated by use of precise time compensation.

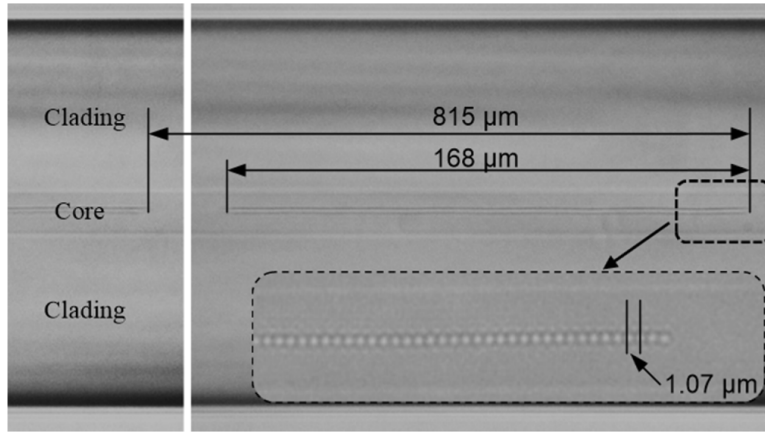


Fig. 2. Optical microscope image of an SFBG fabricated by the fs-laser PBP inscription system illustrated in Fig. 1. The inset presents a high-magnification image of a grating segment. For this SFBG, the number of sampling segments N and duty cycle T are set as 10 and 0.20, respectively, and the measured values of the sampling length L_p and grating segment length L_a are $815 \mu\text{m}$ and $168 \mu\text{m}$, respectively.

The spectral properties of the SFBG shown in Fig. 2 were measured by an optical spectrum analyzer (OSA; Yokogawa Electric Corp., YQAK6319), and are given in Fig. 3(a), where the transmission and reflection spectra are denoted by the red and blue lines, respectively. The figure presents eight obvious peaks in the reflection spectrum, where the wavelength interval between any two adjacent peaks is ~ 1 nm and the depth of the central transmission dip is ~ 4 dB with a bandwidth of ~ 0.2 nm. The reflectivity values of the side-lobe peaks gradually decrease with increasing separation from the central peak. On the short wavelength side, the sideband resonances are not significant because of the overlap with the cladding mode resonance. Details concerning the spectral properties are summarized in Table 1. The polarization-dependent loss (PDL) of the SFBG was measured by an optical component analyzer, which was comprised of a tunable laser source (Agilent, 81940A), polarization synthesizer (Agilent, N7786A), and an optical power meter (Agilent, N7744A). Two orthogonal linear states of polarization corresponding to the grating are displayed in Fig. 3(b). The Bragg wavelength difference of the transverse electric (TE) and transverse magnetic (TM) modes was measured as ~ 0.08 nm, which yields an effective birefringence on the order of 0.75×10^{-4} . A maximum PDL of ~ 2.1 dB was measured at 1547.5 nm, and the significant PDL results from the ellipsoidal index modulation profile induced by the fs laser focusing effect [18].

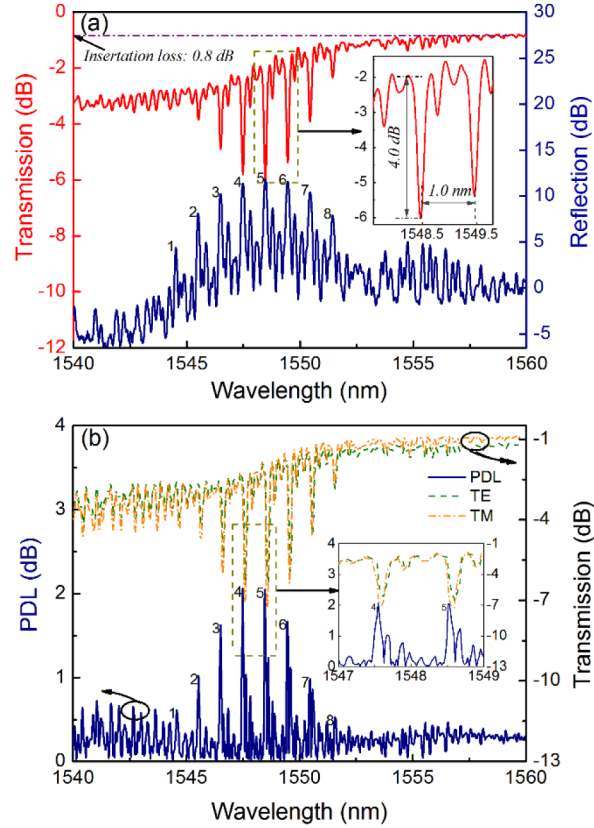


Fig. 3. (a) Transmission and reflection spectra of the SFBG shown in Fig. 2. The inset provides the details of the central peak. (b) The PDL and transmission spectra for two orthogonal states of the SFBG, where the inset image provides the details of the central peak.

Table 1. Parameters of the eight resonance peaks

Peak No.	1	2	3	4	5	6	7	8
FWHM (nm)	—	—	—	0.19	0.21	0.21	—	—
Resonance wavelength (nm)	1544.5	1545.5	1546.5	1547.5	1548.5	1549.5	1550.4	1551.4
Depth (dB)	0.6	1.2	2.3	3.5	4.1	4.0	2.7	1.3
PDL (dB)	0.6	1.0	1.6	2.1	2.0	1.6	1.0	0.5

The SFBG can be analyzed as a cascade combination of several short Bragg gratings. Using the transfer-matrix method [19], the reflection $F_{B,k}$ of each short grating section S_k , $k = 1, 2, \dots, N$, is expressed as follows.

$$F_{B,k} = \begin{bmatrix} \cosh(\gamma_B L_a) - i \frac{\hat{\sigma}}{\gamma_B} \sinh(\gamma_B L_a) & -i \frac{\kappa}{\gamma_B} \sinh(\gamma_B L_a) \\ i \frac{\kappa}{\gamma_B} \sinh(\gamma_B L_a) & \cosh(\gamma_B L_a) + i \frac{\hat{\sigma}}{\gamma_B} \sinh(\gamma_B L_a) \end{bmatrix} \quad (1)$$

Here, κ and $\hat{\sigma}$ are the so-called alternating current and direct current coupling coefficients, respectively, and γ_B is defined as $\gamma_B = \sqrt{\kappa^2 + \hat{\sigma}^2}$. Light propagating through the un-modulated area between each grating segment only experiences a phase shift, which yields a transfer matrix of the following form.

$$F_u = \begin{bmatrix} \exp(-i\phi/2) & 0 \\ 0 & \exp(i\phi/2) \end{bmatrix} \quad (2)$$

Here, ϕ is the phase shift, which can be expressed as $\phi = \beta * L_p$, where β is the propagation constant of the fiber. Based on Eqs. (1) and (2), the reflection of the SFBG can be expressed according to the transfer matrix as

$$F = F_{B,N} \cdot F_u F_{B,N-1} \cdots F_{B,k} \cdots F_{B,2} \cdot F_u \cdot F_{B,1} \quad (3)$$

Several SFBGs with $L = 8.0$ mm and with different values of N , T , and L_p were fabricated, and Eq. (3) was employed to calculate their reflection spectra. The measured and calculated reflection spectra are compared in Fig. 4(a)-4(c), where the solid lines denote the measured reflection spectra and the dashed lines represent the calculated spectra. Figure 4(a) shows the reflection spectrum of an SFBG with $T = 0.20$, $L_p = 0.80$ mm, and $N = 10$. In Fig. 4(b), T is decreased to 0.10 with all other parameters held constant, and we observe that the energy spreads to the surrounding peaks, and more sideband peaks emerge when T is decreased. This can be explained by spatial Fourier transform theory, where the reflection envelop is governed by the sampling function [20]. In Fig. 4(c), L_p is increased to 1.0 mm, N is decreased to 8, and T is returned to a value of 0.20. Comparing the results of Figs. 4(a) and (c), we observe that the wavelength spacing between two adjacent peaks is reduced with increasing L_p . This observation is coincident with previously published results [21]. In Figs. 4(a)-4(c), the experimental spectra generally agree well with the theoretical spectra, although some side lobes of the measured data are either lower or missing with respect to the theoretical results. The explanation for this finding is that higher order side lobes are strongly dependent on the sampling envelop, but the exact shape of the grating structure is difficult to ascertain in the experiment [20]. Clearly, Fig. 4(a)-4(c) demonstrates the good repeatability and controllability of the proposed SFBG fabrication method, and supports a detailed analysis of their thermal properties.

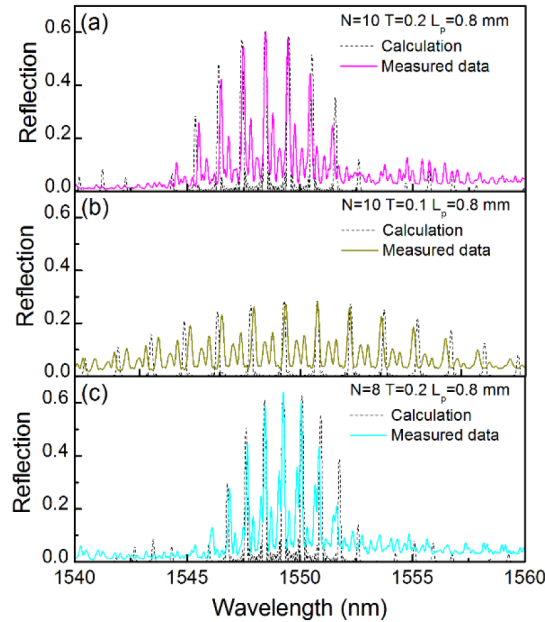


Fig. 4. Calculated and measured reflection spectra of SFBGs with 8.0 mm lengths and different numbers of sampling segments N , duty cycles T , and sampling lengths L_p .

Evaluation of the thermal stability of fs-laser PBP inscribed SFBGs was conducted using the isochronal annealing approach. To this end, the SFBG analyzed in Fig. 4(c) was placed into a tube furnace (Carbolite MTF 12/38/250) capable of attaining temperatures as high as 1200°C. The grating was loosely placed in the furnace to eliminate the application of any external stress. During testing, the central reflection peak was monitored in real time by use of an OSA. The temperature was firstly increased from 100°C to 1000°C, and then decreased back to 100°C in increments of 100°C. The grating spectrum was measured after the temperature at each step was maintained for 10 min. Figure 5 shows the observed variation in the reflectivity and peak wavelength of the SFBG during the heating and cooling processes. The wavelength shift is linearly proportional to the temperature change with a sensitivity of ~ 14.1 pm/°C. The reflectivity fluctuated at a range of 0.8 dB during the heating process and it exhibits little decay during the cooling processes.

A long-term thermal stability test for the SFBG was also conducted by heating the grating to 800°C, and then maintaining that temperature for 6 h. During this process, the results obtained (not shown) demonstrated a 0.5 dB of degradation in the grating reflectivity [22, 23]. The SFBG was subsequently heated to 1000°C and maintained at that temperature for 8 h while the evolution of the grating reflectivity and the resonance wavelength were recorded, as shown in the inset of Fig. 5. A very minor degradation in grating reflectivity of less than 0.5 dB was observed, which represents a thermal stability performance comparable to that of type II-IR gratings [24–26].

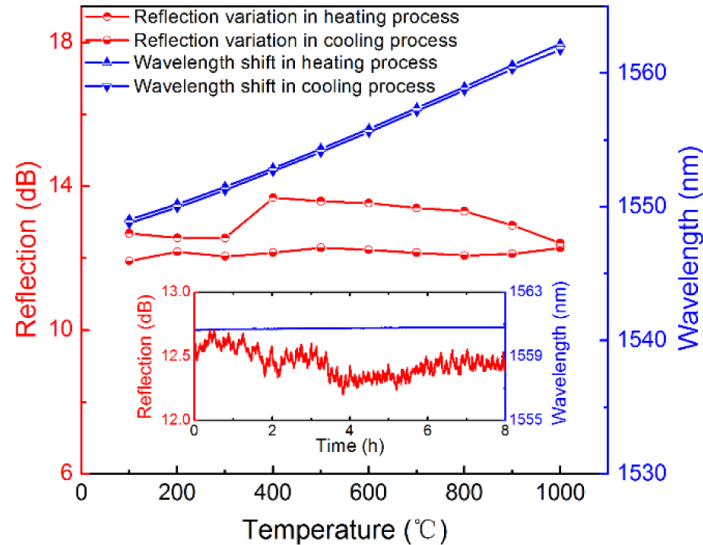


Fig. 5. Variation in the wavelength and reflectivity of the central peak with respect to the surrounding temperature. The inset shows the isothermal evolution of the wavelength and reflectivity of the SFBG over an 8 h period at 1000°C.

Figure 6 shows the reflection spectra of the original state at room temperature, and that after being annealed for 8 h at 1000°C. No significant deterioration in the spectral profile is observed, except for the wavelength shift induced by the high temperature. Clearly, both the central and sideband peaks exhibit great thermal stability.

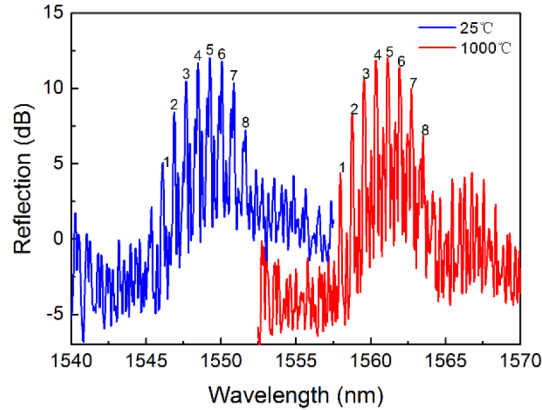


Fig. 6. Reflection spectra of the original state at room temperature and that after annealing for 8 h at 1000°C.

3. Conclusion

In conclusion, we have fabricated a series of SFBGs with easily adjustable sampling periods and duty cycles by use of a 800 nm fs-laser PBP inscription, and their thermal stability was investigated using an annealing approach. The fabricated SFBGs exhibited outstanding thermal stability at temperatures as high as 1000°C. These results demonstrate the potential of the developed SFBGs for use in multi-wavelength fiber lasers and a variety of high temperature applications.

Acknowledgments

This work was supported by National Natural Science Foundation of China (NFSC) (Grant Nos. 61425007, 61377090, 61575128, 61308027, 61405125), Guangdong Provincial Department of Science and Technology (2014A030308007, 2014B050504010, 2015B010105007, 2015A030313541, 2014A030312008), Science and Technology Innovation Commission of Shenzhen/Nanshan (ZDSYS20140430164957664, KC2014ZDZJ0008A, GJHZ20150313093755757, KQCX20140512172532195), Pearl River Scholar Fellowships.